SCIENTIFIC REPORTS

OPEN

SUBJECT AREAS:
CELLULAR NEUROSCIENCE
NEUROIMMUNOLOGY
NEUROCHEMISTRY
BIOMEDICAL ENGINEERING

Received
19 March 2013

Accepted
26 June 2013

Published
24 July 2013

Correspondence and requests for materials should be addressed to S.-H.O. (sang@umn.edu) or M.R. (rodriguez.moses@mayo.edu)

* These authors contributed equally to this work.

A patterned recombinant human IgM guides neurite outgrowth of CNS neurons

Xiaohua Xu[1]*, Nathan J. Wittenberg[2,3]*, Luke R. Jordan[2,3], Shailabh Kumar[2,3], Jens O. Watzlawik[1,4], Arthur E. Warrington[1], Sang-Hyun Oh[2,3] & Moses Rodriguez[1,4]

[1]Department of Neurology, Mayo Clinic College of Medicine, Rochester, MN 55905 USA, [2]Laboratory of Nanostructures and Biosensing, Department of Electrical and Computer Engineering, University of Minnesota, Minneapolis, MN 55455 USA, [3]Department of Biomedical Engineering, University of Minnesota, Minneapolis, MN 55455 USA, [4]Department of Immunology, Mayo Clinic College of Medicine, Rochester, MN 55905 USA.

Matrix molecules convey biochemical and physical guiding signals to neurons in the central nervous system (CNS) and shape the trajectory of neuronal fibers that constitute neural networks. We have developed recombinant human IgMs that bind to epitopes on neural cells, with the aim of treating neurological diseases. Here we test the hypothesis that recombinant human IgMs (rHIgM) can guide neurite outgrowth of CNS neurons. Microcontact printing was employed to pattern rHIgM12 and rHIgM22, antibodies that were bioengineered to have variable regions capable of binding to neurons or oligodendrocytes, respectively. rHIgM12 promoted neuronal attachment and guided outgrowth of neurites from hippocampal neurons. Processes from spinal neurons followed grid patterns of rHIgM12 and formed a physical network. Comparison between rHIgM12 and rHIgM22 suggested the biochemistry that facilitates anchoring the neuronal surfaces is a prerequisite for the function of IgM, and spatial properties cooperate in guiding the assembly of neuronal networks.

Interactions between cells and the extracellular matrix (ECM) determine cell behavior. During development of the central nervous system (CNS), ECM molecules exert both biochemical and physical guidance to shape the trajectory of neural circuits and formation of synaptic connections with target cells. Studies in developmental neurobiology mostly focus on biochemical characterization of signaling induced by guidance molecules. Some chemotactic molecules have been elucidated in governing construction of neuronal networks, which include diffusible and membrane-bound signaling molecules such as netrins, slits, semaphorins, ephrins and some neurotrophins[1]. In addition, bioengineering principles have also been employed to study neural growth[2–4]. An increasing number of materials, synthetic or natural, have been explored, where the biochemical and physical properties are studied to stimulate neuronal adhesion and neurite outgrowth[5].

ECM molecules such as laminin and collagen have been used *in vitro* to make two- or three-dimensional (3D) matrices attempting to promote neuronal growth. Neurites randomly elongate in the 3D matrix and assessment of axonal extension and fasciculation is difficult because of poor spatial resolution[6]. Neurons cultured on uniform 2D surfaces follow a typical style of differentiation[7] and do not reveal how spatial patterns affect axonal development. Nano- or micro-spatially patterned matrix proteins have been employed to test parameters that facilitate cell adhesion and differentiation[8]. Similar to other cell types, neurons and their processes respond to specific spatial patterns[9]. However, the biochemical and spatial cues do not function independently. A functional protein that interacts with neuronal adhesion molecules can support neuron adhesion on specifically designed surface patterns[10]. The specifically modified surfaces could be used to control neuronal growth or as supporting layers for neuron-based biosensors[11,12]. How biochemical and spatial factors cooperate to regulate neuronal behavior is not very well addressed. When designing biomaterials to repair the damaged neural tissue, strategies combining both properties should be considered to improve the survival, proliferation and differentiation of neural cells[13].

Antibodies are a class of natural molecules that are structurally similar, but present specific and versatile binding capabilities. The variable region, composed of 110–130 amino acids, includes the ends of the light and heavy chains and varies greatly among different antibodies through somatic recombination. This feature determines the binding specificity and versatility of antibodies. In contrast, the constant regions for a certain type of antibody have almost identical structural domains because of the similar amino acid sequences. IgM antibodies are mostly presented as pentamers of five immunoglobulins that are covalently linked together with disulfide bonds. The pentameric IgM is a large molecule with a molecular weight of about 900 kDa and has 10

antigen-binding sites[14]. Thus the pentameric IgM, compared to its monomeric counterpart, has much higher avidity towards its antigen(s). This structural feature makes IgM an ideal molecule in elucidating how biochemical and physical properties cooperate in the spatio-temporal context when arranged into specific spatial patterns. We previously showed that a human natural IgM, when attached to nitrocellulose on a glass substrate, promoted axonal outgrowth[15]. How the chemical and physical properties of the IgM function to promote axonal extension is currently under investigation.

A common method for patterning biomolecules on solid substrates is microcontact printing (μCP). Microcontact printing is an application of soft lithography that employs poly(dimethylsiloxane) (PDMS) elastomer stamps with patterned features to print molecules on a surface[16]. The initial application of μCP by Whitesides and coworkers was to pattern self-assembled monolayers of alkanethiolates on gold surfaces[17]. These alkanethiol patterns were subsequently used for selective adsorption of extracellular matrix molecules to pattern attachment and growth of hepatocytes[8]. Since then, μCP has been used to define patterns of biomolecules, including peptides, antibodies[18], nucleotides and many types of extracellular matrix molecules. Earlier studies indicate that while antibodies patterned by μCP may lose some immunological functions, their specificities remain unchanged[19]. μCP-generated patterns can support the growth of a wide variety of cell types, including epithelial cells, hepatocytes, adrenal cells and neurons[20]. An advantage for using μCP for neuronal cultures is that as axons grow they will follow the patterns of printed molecules and make functional synaptic connections[21]. Moreover, user defined concentration and spatial gradients of immobilized molecules can be used to direct axon growth[22]. To guide the growth of neurons, extracellular matrix molecules, such as laminin and poly-d-lysine are commonly patterned[23,24].

In this report, recombinant human IgMs were patterned onto glass substrates by μCP and growth behavior of CNS neurons was studied. A uniformly patterned rHIgM12 promoted neuronal attachment, while rHIgM12 patterned in a concentration gradient guided the neurite navigation of hippocampal neurons. Neurites of spinal neurons followed grid patterns of rHIgM12 and elongated forming a physical network. Our results indicated that the patterned human IgM can guide neurite outgrowth. Both biochemical and spatial characteristics were required in guiding neurite extension, though the chemical identity played a major role in promoting neurite outgrowth. Patterns of another recombinant antibody that has the same constant domain but binds to oligodendrocytes (rHIgM22)[25,26] did not promote neuronal attachment or neurite extension. The chemical features of rHIgM12, when presented in a chemical gradient or arrayed in a fibrillar pattern, were sufficient to convey guidance cues to determine the direction of neurite outgrowth.

Results

Patterning recombinant human IgMs by microcontact printing. Patterns of human IgM and other molecules were transferred to clean, unmodified glass substrates by μCP. The μCP stamps had square, line, grid and ring patterns. A schematic illustration of the μCP process is shown in Figure 1A. Figure 1B shows a grid pattern of human IgM after incubation with a fluorescein-conjugated anti-human secondary antibody. The grid lines were approximately 20 μm wide. The printed patterns were generally uniform over large (~mm^2) areas. Without chemical modification of the glass substrates, transfer of the IgM patterns to the glass surface was mediated by noncovalent interactions. The exact nature of the IgM-glass interactions and orientation of the IgMs on the glass is unknown at this time. The IgM patterns persisted after a number of washing steps, which indicates the patterns were sufficiently stable for *in vitro* experiments. Two recombinant human IgMs, rHIgM12 and rHIgM22 which were selected based on their binding to either neurons[15] or oligodendrocytes[25,26], were used in this study. Their binding specificity to neurons or oligodendrocytes was further confirmed in Figure 1C & D. Constant domains of the two IgMs were bioengineered to have the identical amino acid sequences while the variable regions binding to epitopes on either neurons or oligodendrocytes were kept intact. Immunocytochemistry images show that rHIgM12 and rHIgM22 maintained the capability to bind to the surfaces of neurons or oligodendrocytes. Thus, the biochemical features in the variable region were hypothesized to determine the neuronal behavior when the IgMs were printed to the same spatial patterns and the effect of different patterns composed of the same IgM backbone can also be compared.

The IgM patterns were further characterized by atomic force microscopy (AFM). Figure 1E shows the AFM images and line profiles of the intersection point on grid patterns of rHIgM12 and rHIgM22. The line profile shows that the thickness of the stamped antibody patterns typically averaged between 10–20 nm. Both the immunochemistry and AFM images indicated that the grid patterns were printed with high fidelity.

Biochemical features of IgM determine neuronal attachment and neurite outgrowth. To test how the biochemical features of IgMs independent of spatial patterns affected neuronal behavior, both rHIgM12 and rHIgM22 were printed uniformly on a glass substrate as a continuous 2D sheet without forming a specific pattern. We predicted that spatial cues that would guide neurite outgrowth could be eliminated when the IgM was printed uniformly on the 2D surfaces. Embryonic day 15 hippocampal neurons were seeded on these substrates. At 3 days *in vitro* (DIV3), the neurons were fixed and stained with anti β3-tubulin antibody that specifically labeled the cytoskeletal microtubules in neurons. The human IgMs were labeled with anti-human IgM secondary antibodies, and the nuclei by DAPI. As indicated in Figure 2A & B, a significantly larger number of neurons attached to the substrates with rHIgM12. Cellular attachment indicates that the μCP process does not significantly affect the specificity of rHIgM12 for neuronal surface antigens. Neurons growing on rHIgM12 showed robust β3-tubulin positive neurites oriented randomly within the 2D territory of rHIgM12. In comparison, the neurons that attached to either rHIgM22 or regions without IgM had few neurites. Neurons that attached to the substrates were further quantified by measuring the fluorescence intensity. Three regions from each coverslip were randomly selected and the fluorescence intensities were averaged based on the sizes of the area. Figure 2C shows the quantified results. The averaged intensities of both DAPI and β3-tubulin from neurons grown on rHIgM12 were significantly higher than that of neurons on rHIgM22. These results indicated that rHIgM12 promoted both neuronal attachment and neurite outgrowth when printed on a 2D surface. It also suggested that the IgMs withstood the μCP transfer process and maintained their specificity and bioactivity. The significant contrast between rHIgM12 and rHIgM22 on neuronal growth further suggested that it was the biochemical properties of the IgM variable regions that determined neuronal attachment and neurite outgrowth.

A Gradient of rHIgM12 can guide neurite migration. Many studies showed that guidance molecules that shape the direction of neural navigation also affect neurite outgrowth[27]. We then examined if rHIgM12, when presented in a gradient fashion, can similarly regulate the projection of neurites. To create a gradient of rHIgM12, 500 μL of rHIgM12 solution was loaded on the top of a PDMS stamp and a mild nitrogen flow was applied from one side of the stamp. Thus, a relative gradient of rHIgM12 was created on the stamp and the adsorbed rHIgM12 gradient was then transferred to a cover glass by μCP as shown in Figure 3A1. Figure 3A2 shows a plot of the fluorescence intensity from the human IgM secondary antibody suggesting that the gradient of rHIgM12 was successfully transferred onto the coverslip. In Figure 3A2, the fluorescence intensity of rHIgM12 steadily increased from left to right, starting

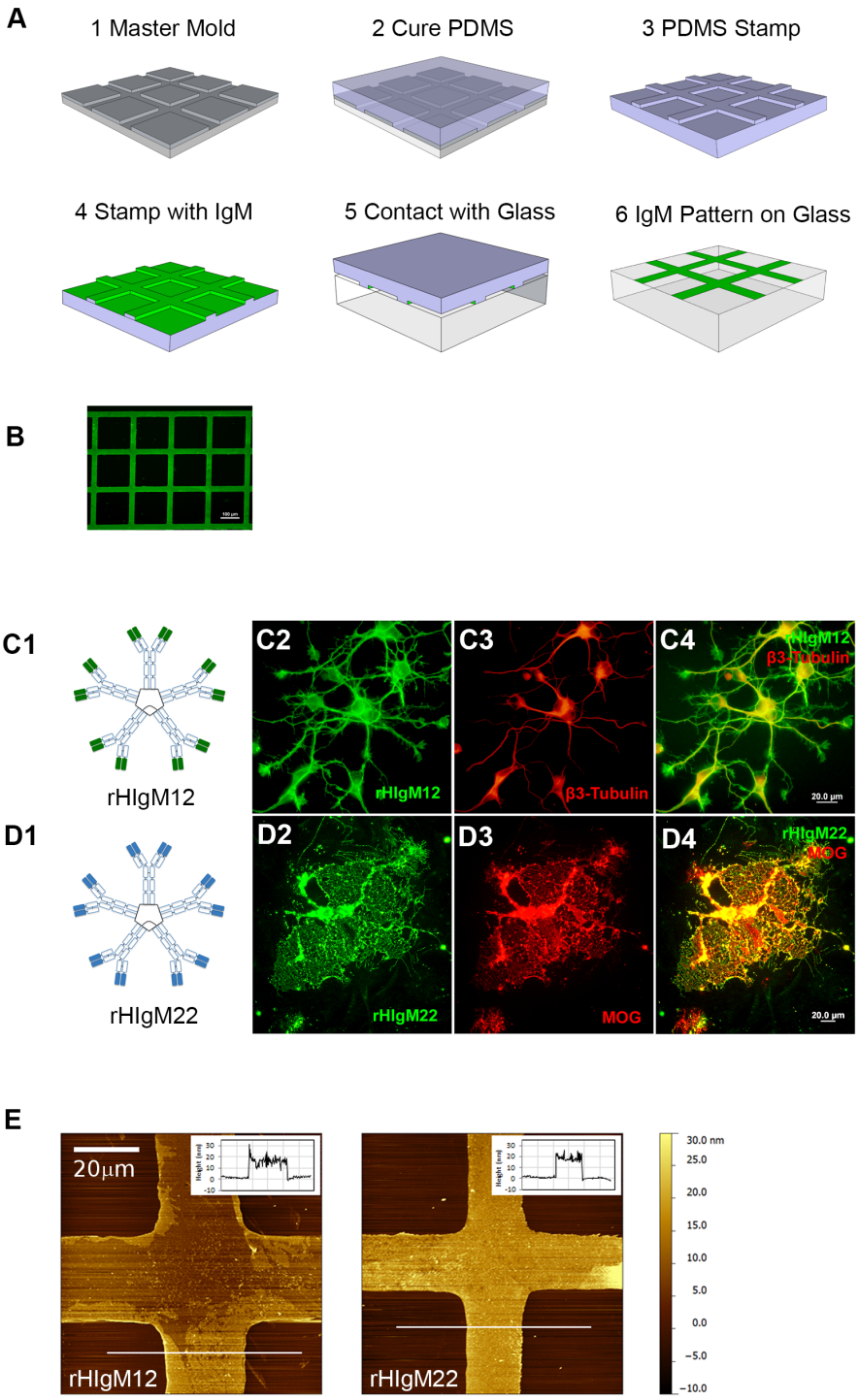

Figure 1 | Microcontact printing of recombinant human IgM and AFM imaging. (A). Schematic illustration of the μCP process. First, a master mold with inverse features from the desired μCP stamp was fabricated (1). PDMS liquid was then cast upon the master mold, allowed to cure (2) and then the stamp was peeled away from the master mold (3). Next the stamp was "inked" with an antibody solution (4). Finally, the patterns were transferred to the glass substrates by placing the stamp in contact with a clean glass coverslip (5). The stamp was peeled off, leaving behind patterns of IgM (6). (B). A grid pattern of rHIgM22 labeled with fluorescein-conjugated anti-human IgM antibody. (C, D). Immunocytochemistry images showed that rHIgM12 and rHIgM22, which had the same constant domains but were different in the variable regions, bound to epitopes on neurons (C) or oligodendrocytes (D). (E). AFM height images of the intersection point of grid patterns of rHIgM12 and rHIgM22. The line profile corresponds to the long horizontal line in the AFM image. Scale bar, 100 μm in (B), 20 μm in (C), (D), and (E).

approximately in the middle of the image. More interestingly, however, the primary neurites (Figure 3B1) migrated parallel to the direction of the rHIgM12 gradient, and a much denser neurite meshwork was observed in regions with higher rHIgM12 density. Comparison of the fluorescence profiles in Figures 3A2 and 3B2 indicates that increased β3-tubulin intensity was coincident with that of the rHIgM12. The DAPI channel (Figure 3C) shows that the nuclei were distributed relative evenly across the patterned rHIgM12 gradient. Quantification of the averaged fluorescence intensities was performed (Figure 3D). Both the rHIgM12 and

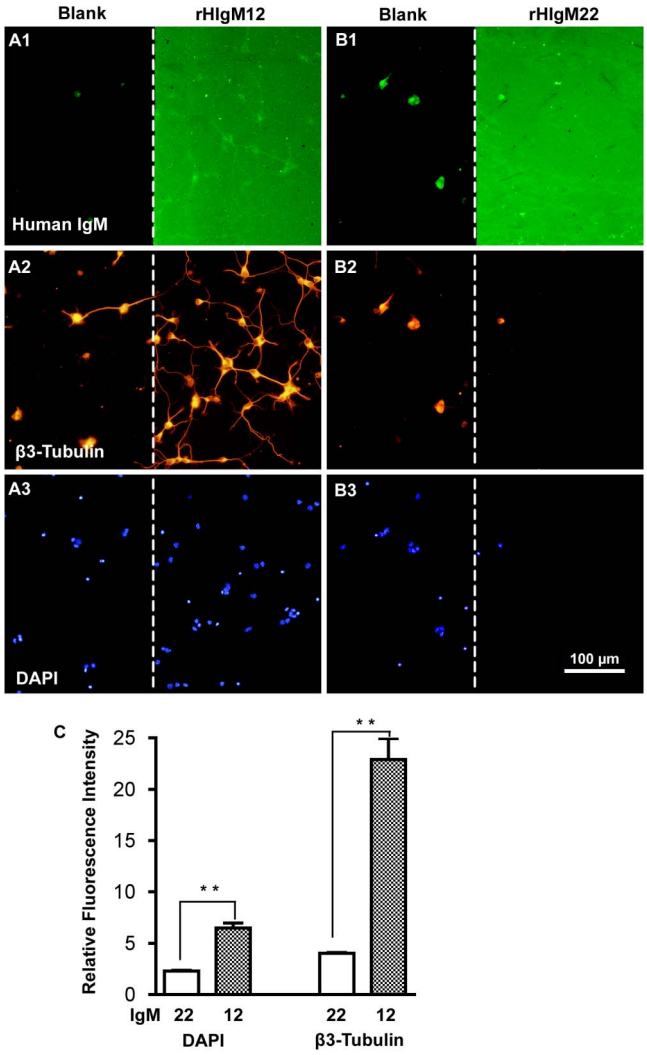

Figure 2 | Uniformly printed rHIgM12 promoted neuronal attachment and neurite outgrowth of hippocampal neurons. rHIgM12 (A) and rHIgM22 (B) were printed on glass substrate in a uniform 2-dimensional pattern. Mouse hippocampal neurons were seeded on the IgM patterns. The DIV3 culture was stained with anti-human IgM secondary (A1–B1), anti-β3-tubulin antibody (A2–B2) or DAPI (A3–C3). (C). Quantification of the averaged fluorescence intensities of DAPI and β3-tubulin ($p < 0.01$, N = 5). Scale bar, 100 μm.

β3-tubulin intensities were significantly higher in the gradient regions of rHIgM12 compared to the uniform regions. The differences in DAPI intensity were not significant, which suggests there is no difference in the number of cells attached to either the uniform or gradient areas. Quantitatively, the number of cells attached to the areas of uniform density of rHIgM12 (10.7 ± 2.3, mean ± S.D., N = 3 images) was not significantly different than the number of cells attached to areas of rHIgM12 gradient (15.3 ± 7.0, N = 3 images) ($p = 0.06$).

We then analyzed the direction of neurite outgrowth relative to the increasing gradient direction. Since areas of uniform rHIgM12 and rHIgM12 gradient were on the same substrate (Figure 3A1-2) we analyzed the growth direction of neurites separately depending upon whether the neurons were attached to uniform (left half of Figure 3B1) or gradient (right half of Figure 3B1) areas. Figure 3E shows angular histograms of neurite outgrowth angle (θ) relative to the direction of the rHIgM12 gradient. On the rHIgM12 gradient, 69.3% of the histogram area lies $< 90^\circ$ or $> 270^\circ$ in contrast to 58.8% in the uniform area. Quantification of neurite outgrowth angles indicated that the angle of deviation from the gradient (ϕ) for neurites projecting from cells on the uniform areas deviated on average $82^\circ \pm 51^\circ$ (mean ± S.D., N = 143 neurites) from the gradient direction, while on gradient areas the neurites on average deviated $67^\circ \pm 46^\circ$ (N = 231 neurites) ($p < 0.01$) (Figure 3F). About 70% of neurites from cells on gradients grew toward higher rHIgM12 concentration. These results suggested that rHIgM12, displayed in a chemical gradient, not only promoted neurite outgrowth but provided guidance cues that induced extending neurites to migrate toward a higher concentration of rHIgM12.

Biochemical and spatial features of the patterned IgM cooperate to guide neurite outgrowth. Guidance cues were found to be spatial-temporally regulated *in vivo*[28]. Different from non-neuronal cells, neuronal processes differentiate into nerve fibers that favor a fibrillar scaffold. Thus we hypothesize that spatial cues affect neuronal growth and differentiation, and that the biochemical and spatial factors of a given guidance molecule are not segregated but cooperate in conveying guidance signals. To examine if spatial cues were also involved in the IgM-mediated guidance of neurite outgrowth, different spatial patterns of IgM were prepared. Neurite outgrowth was first assessed with hippocampal neurons on 'discontinuous' square patterns (80 μm × 80 μm) with a center-to-center distance of 150 μm. By discontinuous we mean that the squares are isolated from one another with no connections between them. Shown in Figure 4A and B, DIV3 neurons plated at the density of 3×10^5 cells/35 mm dish send out neurites which elongate and form an isolated dense meshwork within the territory of patterned rHIgM12 squares and the few neurons that attach to rHIgM22 bore almost no neurites. This observation was similar to the results from neurons grown on the uniform 2D patterns of human IgM that rHIgM12, but not rHIgM22, facilitated neuronal attachment and neurite outgrowth (Figure 2). However, the hippocampal neurons grown at 3×10^5 cells/35 mm dish did not show obvious guidance information conveyed by the patterns *per se*. Axons of many neurons *in vivo* often bundle together to form fasciculations. Neurites from cultured neurons were also tangled when they met with each other on a planar surface. To reduce the potential interaction from neighboring neurons and test if the printed IgM squares can affect neurite extension, we examined DIV1 hippocampal neurons that were seeded at a density of 1×10^5 cells/35 mm dish. Only square patterns of rHIgM12 were used because rHIgM22 did not function to support neuronal attachment and neurite outgrowth. Many neurites elongate around the edge of the patterns, instead of extending over the interior of the rHIgM12 squares (Figure 4C). Neurite preference for pattern edges may be due to the nature of the printed pattern. Slightly thicker rHIgM12 layers were commonly observed on the edges of features, as shown in the AFM image in Figure 1E. These observations suggested that geometrical pattern of rHIgM12 may have an effect on neurite outgrowth, which can be complicated when the neurons were seeded at a higher density and the neurites interacted with each other and were bundled together forming a meshwork.

It has been reported that many types of neuron prefer the fibrillar spatial patterns that guide polarized axonal extension[29–31]. In the spinal cord, axonal fibers of both sensory and motor neurons fasciculate into bundles and are distributed within different regions in the cord periphery. This anatomic character suggests that processes from spinal neurons have the intrinsic ability to fasciculate during development, either naturally or guided by a potential scaffold. In spinal cord injury (SCI), the physiological organization of spinal neurons is destroyed. Glial scars form and the regenerating spinal neurons fail to establish connections with their target cells. SCI therapy may benefit from understanding of the factors that guide spinal neuron growth and differentiation. To explore the rules that mediate neuronal navigation in the spinal cord, we next used cultured spinal

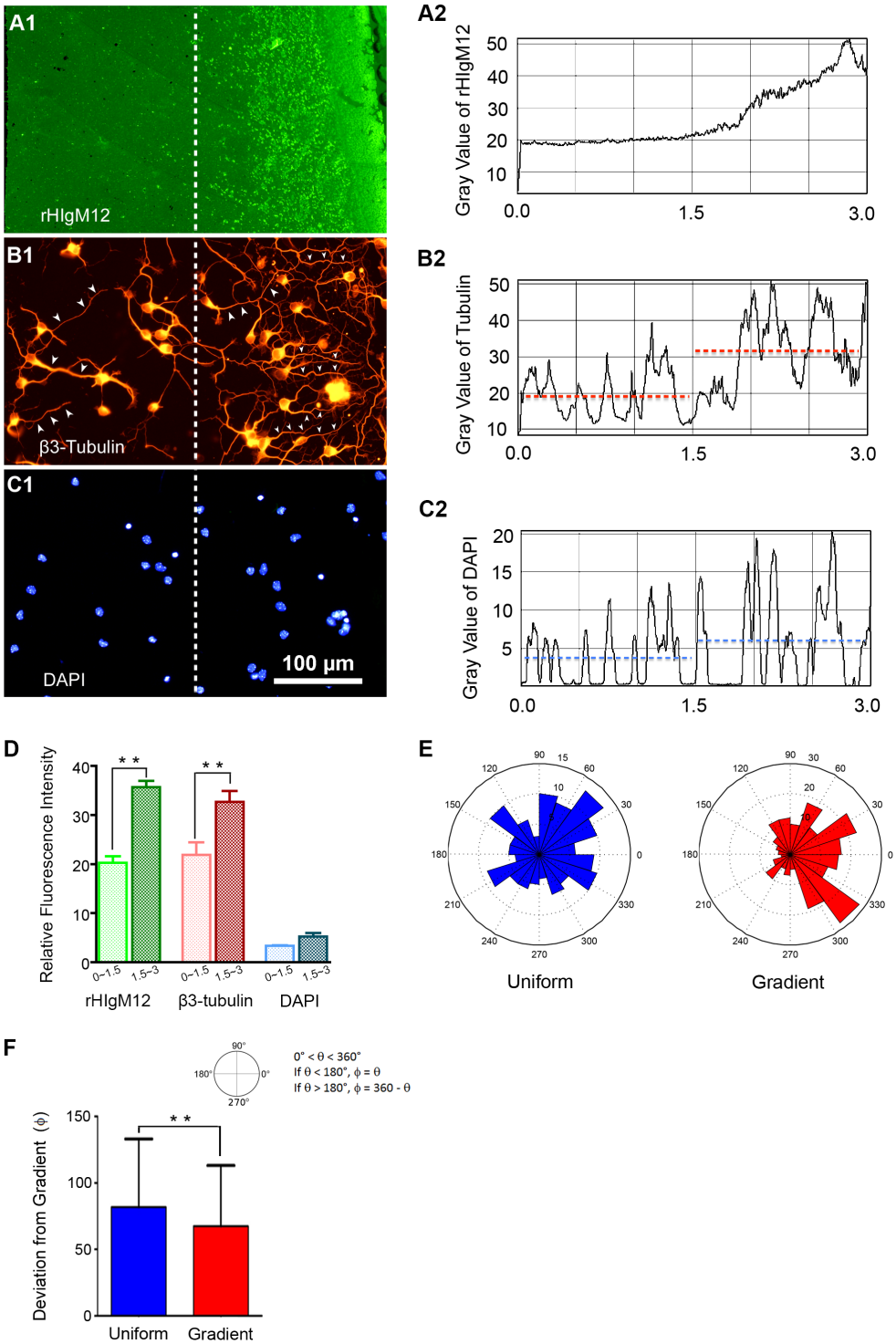

Figure 3 | A gradient of printed rHIgM12 guided neurite projection. (A). A gradient of rHIgM12 was patterned onto the glass substrates (A1) and the plotted fluorescence intensity of rHIgM12 is shown in (A2). The intensity of rHIgM12 was uniform until roughly at the 1.5 inch-mark on the selected regions that were normalized into a 3-inch wide field. After the 1.5 inch-mark the rHIgM12 concentration increased in a left-to-right gradient. (B). In the β3-tubulin channel, the primary neurites (white arrow heads) migrated towards the higher gradient of rHIgM12 (B1) and a dense meshwork of neurites was formed in regions with higher rHIgM12 density. Image (B2) shows the profile of β3-tubulin intensity where the average was indicated by dashed lines from 0 to 1.5 and 1.5 to 3 inch. (C). The nuclei were stained by DAPI. Image (C1) shows the localization of the nuclei and (C2) its profile. (D). Quantification of the averaged fluorescence intensities from the above 3 channels. The bar graph was an analysis from 3 experimental repeats. Both the rHIgM12 and β3-tubulin intensities were significantly higher in regions from 1.5 to 3 inch compared to that in between 0 and 1.5 inch ($p < 0.05$), while the difference on DAPI intensity was not significant ($p = 0.06$). (E). Angular histograms showing the direction of neurite outgrowth (θ) for cells attached to uniform areas of rHIgM12 (from 0 to 1.5 inch in Figure 3A1, blue) or a left-to-right gradient of rHIgM12 (from 1.5 to 3 inch in Figure 3A1, red). On the rHIgM12 gradient, 69.3% of the histogram area lies $< 90°$ or $> 270°$ in contrast to 58.8% in the uniform area. (F). Quantification of outgrowth angles (ϕ; mean ± SD) relative to the gradient direction. The neurites projecting from cells on the uniform areas deviated on average $82° \pm 51°$ (mean ± S.D., N = 143 neurites) from the gradient direction, while on gradient areas the neurites on average deviated $67° \pm 46°$ (N = 231 neurites) ($p < 0.01$). Scale bar, 100 μm.

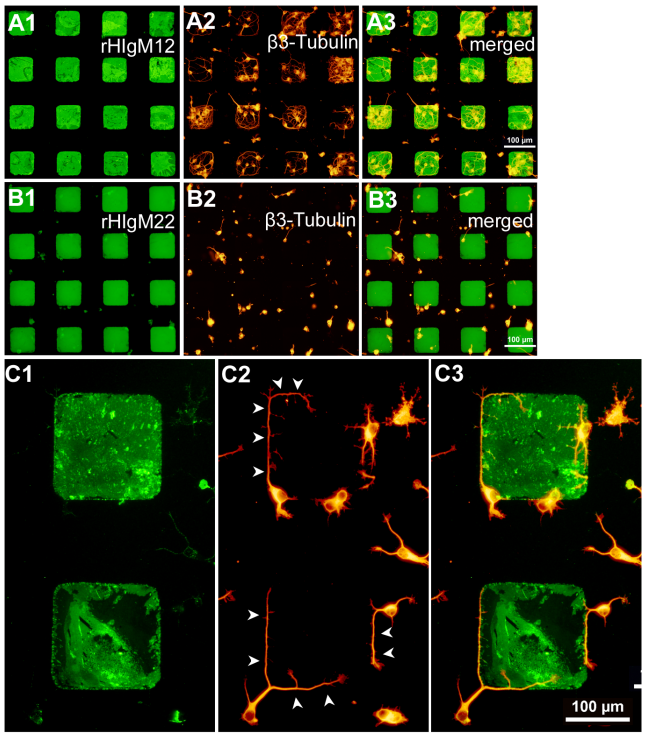

Figure 4 | Neurite outgrowth of hippocampal neurons on discontinuous square patterns of IgM. (A & B). Hippocampal neurons were plated on discontinuous square patterns of rHIgM12 (A) or rHIgM22 (B) with a size of 80 μm × 80 μm and a center-to-center spacing between the squares of 150 μm. The neurons were fixed and stained at DIV3. Green, human IgM. Red, β3-tubulin. Dense meshworks of neurites were formed on the rHIgM12 patterns, while few neurons attached and initiated neurites on rHIgM22. (C). Hippocampal neurons were seeded on rHIgM12 at a density of 1×10^5 cells/35 mm dish and examined at DIV1. Many neurites followed the edge in the periphery of the patterns. Scale bar, 100 μm.

neurons to study how a 2D network pattern can shape neurite extension. Spinal neurons were first seeded at a density of 3×10^5 cells/35 mm dish on patterned IgM grids that had 20 μm wide lines with the node center-to-center distance of 200 μm (Figure 5). As alternatives to the isolated squares used in Figure 4, the grid patterns in Figure 5 were designed to present different spatial cues through the continuous paths that the growing neurites follow. At DIV3, the neurons that survived were stained with anti β3-tubulin antibody. The spinal neurons attach to the rHIgM12 grids and send out robust neurites that bundle together forming a physical network on the rHIgM12 patterns (Figure 5A). Similar results were also observed when the spinal neurons were grown on patterns of laminin plus poly-D-lysine of the same size. (Figure S1 in the Supplementary Information) Together, these results indicated that the continuous rHIgM12 patterns can confer guidance cues. While in contrast, the rHIgM22 patterns of similar size neither supported neuronal attachment nor facilitated neurite outgrowth (Figure 5B), further strengthening the crucial role of the IgM variable region in neurite outgrowth.

The results in Figure 4A and 5A indicated that spatial patterns did shape the neuronal projection. To further test if rHIgM12 conveyed guidance cues positively as suggested in Figure 4C, a ring pattern of rHIgM12 was generated. Rather than straight lines and right angles, ring patterns present a continuous curvature. The neuronal behavior was examined by plating the spinal neurons at a lower density of 1×10^5 cells/35 mm dish. As shown in Figure 5C, spinal neurons at DIV5 project their neurites along the inner and outer edges of the ring-shaped rHIgM12 patterns. This observation demonstrated that the spinal neurons do not just passively follow, but positively respond to

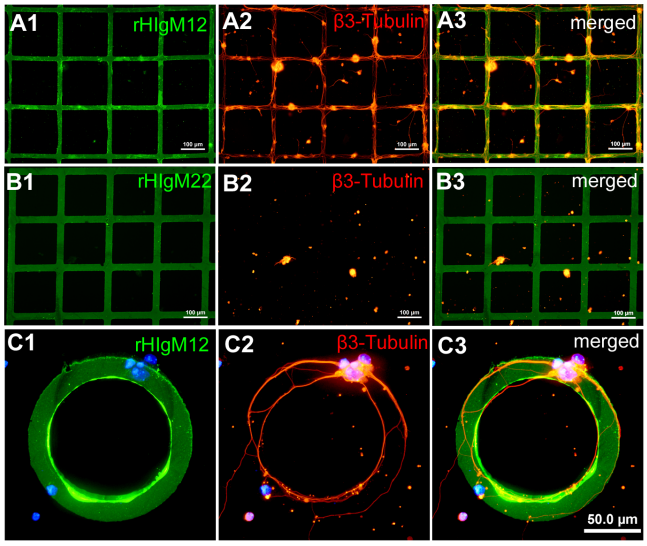

Figure 5 | Neurite outgrowth of spinal neurons on the continuously patterned IgM. (A & B). Spinal neurons were seeded on grid patterns of rHIgM12 (A) or rHIgM22 (B) that had ~20 μm-wide lines with the node spacing of 200 μm. At DIV3, the attached neurons sent out robust neurites that followed the rHIgM12 grids forming a physical network, while few neurons attached and initiated neurites on rHIgM22. (C). Image showing the behavior of spinal neurons at a lower density of 1×10^5 cells/35 mm dish. At DIV5, the neurites migrated along the inner and outer edges of the ring rHIgM12 patterns. Scale bar, 100 μm in (A & B), and 50 μm in (C).

the rHIgM12 spatial patterns. The results from both rHIgM12 and rHIgM22 also suggested that the biochemical and spatial features of the patterned IgMs cooperated to guide neurite elongation.

Discussion

We have shown that μCP is an effective method to generate patterns of recombinant IgM antibodies, and that one antibody, rHIgM12, can guide neurite outgrowth from CNS neurons. In using AFM to characterize the printed antibody patterns we found that the antibody layer was usually between 10 and 20 nm thick. (Figure 1E) Previous reports on AFM and scanning electrochemical microscopy characterization of IgG antibody patterns have shown layers that were roughly 5 nm thick, indicating that monolayers of IgG antibodies lay flat on glass[32] or mica[33]. IgM molecules have a distinctly different structure than IgGs. IgMs are shaped like five-armed stars, with five Fc domains converging at a central linkage point via disulfide bonds. Molecular modeling calculations suggest that IgMs are not flat, but rather are mushroom-shaped in order to facilitate key disulfide linkages between the Fc domains of five IgM monomers[34]. This prediction was experimentally confirmed using cryogenic AFM[34]. The mushroom-like 3D structure of IgMs may explain why the antibody patterns in this study were thicker than μCP generated patterns of IgG antibodies.

Many materials, including ECM proteins, have been patterned on solid substrates by μCP aimed to study cell attachment and growth. How human IgMs bind to neural cells and regulate their behavior is an emerging domain of research[35]. Because of the molecular complexity, the interactions between IgMs and their target cells are likely complicated. When the V domain at the tips of the F(ab) binds to epitopes on neural cell surfaces, the Fc parts can activate Fc receptors or complements. Thus the function of IgM molecule *in vivo* depends on a spatio-temporal context. We previously attached rHIgM12 to a layer of nitrocellulose on a glass substrate and showed that the IgM supported axonal outgrowth[15]. However, adsorption of IgM to nitrocellulose was random with respect to the orientation of the IgM

molecules. Here we employed the technique of μCP and successfully patterned IgM molecules on the solid glass substrate. Without chemical modification, IgMs do not form covalent bonds with the glass substrate. However, it seems the noncovalent interactions between IgM and glass that mediate adsorption do not cause deleterious effects and reduced IgM function.

IgM is the first immunoglobulin produced by the developing B-type lymphocytes (B-cells). Monomeric IgM can be expressed on naive B-cell surfaces. In mature or antigen-stimulated B-cells, IgMs are secreted mostly as pentameric and rarely hexameric forms linked by disulfide bonds in the 4th C-domain of the heavy chain. The pentameric IgM also contains a joining polypeptide, the J-chain, which binds to 2 of the monomers by disulfide bonds. The J-chain is a relatively conserved polypeptide which is incorporated into the polymeric IgM and facilitates its secretion. Another proposed function of the J-chain is to hinder complement binding and negatively affect cytolytic activity of the polymeric IgM[36]. The IgMs used in the current study were bioengineered recombinant human immunoglobulin in which rHIgM22 was generated first and contained a mouse J-chain, whereas rHIgM12 was made later and had a human J-chain instead. By comparison of amino acid sequences, the human and mouse J-chains were shown to be 77% identical and the structures involved in polymerization were mostly conserved[37]. Thus when both of the IgMs were used *in vitro*, the J-chains were less likely to affect the IgMs' binding activity, which were usually determined by the V domain. The binding specificity of the IgMs to neural cells shown in Figure 1C & D and Figure 2A & B further confirmed this point, either dissolved in solutions or micro-printed on the glass surfaces. The C domains of the heavy chain (C_H) in each monomer IgM can fold into a constant structure consisting of 4-stranded β-sheet pinned together by an intrachain disulfide bond. The C_H1 domain is located within the F(ab) region, whereas the rest of C_H domains ($C_H2{\sim}4$) comprises the Fc fragment which mediates effector function either by binding to the Fc receptors or activating complements. Thus changes in the Fc region can finally affect the antibody function *in vivo*[36]. In our study, the C domains of rHIgM12 and rHIgM22 were bioengineered to have the same amino acid sequences and both were used *in vitro* as spatial patterns. Thus, when both rHIgM12 and rHIgM22 were printed to form the same spatial microstructures, their physical properties would be very similar and only the V regions would determine their biological function. Imaging with AFM (Figure 1E) also indicated that printed rHIgM12 and rHIgM22 both have thicknesses between 10–20 nm. In our preliminary experiments with the serum-derived IgMs that all have human J chains, identical responses as the purified recombinant ones were observed. In the subsequent experiments, only the purified recombinant IgMs were used because they were of higher purity than the serum IgMs. As indicated in the method, the recombinant IgMs were 97% pure and were also used in an animal model of multiple sclerosis to promote remyelination[38]. Taken together, we conclude that the observed neuronal response is determined by the V region of the IgM in collaboration with the given spatial organization. Thus rHIgM12 and rHIgM22 presented the best pair to study how the biochemistry and physical properties of IgM could affect neurite outgrowth.

When printed in a uniform 2D layer, rHIgM12 but not rHIgM22 supported neuronal attachment and neurite outgrowth, suggesting that V domains of the IgM played a crucial role in determining the biological function. Sparse neurites extend randomly on the uniform rHIgM12 area, while a much dense mesh of neurites grows toward a higher gradient of patterned rHIgM12. Measurement of neurite outgrowth angle showed that the mean angle of deviation is not significantly different from a hypothetical random outgrowth situation, indicating that the neurites on a uniform rHIgM12 do not present significant growth preference (Figure 3E). However, for cells attached to areas that have a rHIgM12 gradient (Figure 3E–F), there is a strong preference of neurite outgrowth toward a higher gradient, i.e. in the direction of increasing rHIgM12 concentration. Thus a gradient of rHIgM12 conveyed powerful guidance cues. The anchored IgMs could also generate a gradient *in vivo* to guide motile cell movement. Membrane-bound guidance molecules and ECM indeed were found to be expressed differentially in the CNS. Cultured neurons *in vitro* were shown to prefer the fibrillar patterns[29] and presented a polarized growth style[39]. These observations indicated that factors arranged into spatial patterns can influence axonal projection. How the biochemical and physical features of a guidance molecule cooperate spatio-temporally is not fully understood and is worth further study. We tried to address this question by utilizing the characteristics of rHIgM12 and rHIgM22 which have the same backbone but different biochemical binding activity. rHIgM22, patterned in the spatial patterns tested in our study, did not support neurite outgrowth, suggesting that the spatial factors alone were not sufficient to support neuronal differentiation. In contrast, rHIgM12 when patterned uniformly or as a discontinuous squared pattern of 80 μm × 80 μm promoted neurite outgrowth, but did not confer obvious directional information to the attached hippocampal neurons. Intriguingly, neurites from single neurons at a lower density did follow edges of the patterned rHIgM12. When the pattern size was reduced to ~20 μm, neurites of attached spinal neurons followed the grid patterns of rHIgM12 and bundled to fasciculate, though the possibility that the pioneer neurites would initially serve as anchoring sites and lead the projection of others cannot be ruled out. Taken together, the spatial patterns on a basis of biochemical affinity do have an effect in guiding neurite extension. Comparison of the effect between rHIgM12 and rHIgM22 indicates that the biochemical and physical features of IgM do not work alone, but cooperate in conveying guidance cues. To our knowledge this is the first demonstration of a human natural antibody guiding neurite outgrowth, however the underlying molecular mechanisms are yet to be determined.

In conclusion, we demonstrated that μCP is an effective method to generate patterns of human IgM. The patterned recombinant IgM, rHIgM12, maintained the bioactivity to promote neuronal attachment and neurite outgrowth. Neurons cultured on gradients of rHIgM12 responded to the gradient by projecting neurites in the direction of higher antibody concentration. Cultured spinal neurons formed physical networks on the IgM grids. Thus, the neuron-binding IgMs can be used to promote formation of neural networks that could be useful for cell-based biosensors and open a new window in regulating neural activity with a potential for clinical utility.

Methods

Recombinant human IgM antibody. rHIgM12 was expressed in CHO cells[15], and rHIgM22 in F3B6 cells[25]. Briefly, the IgM antibodies expressed in the serum of Waldenstrom's macroglobulinemia patients were sequenced. Plasmids expressing the heavy and light chain coding sequences for the predominant antibody were transfected into the target cells. The resulting cells were selected with increasing doses of methotrexate, and a stable clone that produced the antibody as measured by ELISA was subcloned and expanded. The recombinant IgM in culture supernatant was purified by chromatography to 97% as measured by HPLC analysis in a GMP facility approved by the FDA.

Soft lithography. A silicon master mold for the PDMS stamps was prepared at the University of Minnesota Nanofabrication Center. SU-8 50 negative photoresist was spin-coated over a silicon wafer to achieve a final thickness of 40 μm. The wafer was then exposed to ultraviolet light through a chrome mask and washed with propylene glycol monomethyl ether acetate which acts as a developer. The wafer was then treated with trichloro (1*H*, 1*H*, 2*H*, 2*H*-perfluorooctyl) silane, which forms a self-assembled monolayer on the surface and helps in detachment of cured PDMS. The PDMS stamps were prepared using Sylgard 184 elastomer (Dow Corning). The elastomer was mixed in 10 : 1 ratio (w/w) with curing agent and was degassed for 30 minutes to remove any air bubbles from the mixture. This mixture was then poured over the silicon master mold and placed on a hot plate (70°C) overnight. The stamps were cut carefully from this mold and submerged in 50% ethanol for cleaning.

Microcontact printing. Matrices used for neuronal culture were microcontact-printed onto Fisher glass coverslips. Briefly, glass coverslips were treated in 1 M HCl

or HNO_3 at 60°C for 16 hours in a glass beaker. After cooling to room temperature, the coverslips were sequentially washed first with deionized, then Milli-Q water. The extensively washed coverslips were rinsed with ethanol and stored in ethanol before use. Before μCP, the coverslips were blown dry under a nitrogen flow. The stamps were inked with antibodies dissolved in phosphate buffered saline (PBS) pH 7.4 by placing large drops on the stamps for 45 minutes. After incubation, the stamps were washed three times with Milli-Q water, and then blown dry under the nitrogen flow. The stamps were then placed in contact with the coverslips, taking care not to shift position of the stamp after contact. After 30 minutes of contact with the coverslip, the stamps were slowly detached. The glass coverslips with different patterns were washed three times with PBS and then incubated with neuronal culture media containing Neurobasal™ plus 2% (v/v) of B27 in a 37°C CO_2 incubator.

Neuronal culture and immunocytochemistry. Both hippocampal and spinal neurons from FVB mice (The Jackson Laboratory, ME, USA) were used in the experiments. Primary spinal neurons were prepared from embryonic day 11 to 13 mice. Briefly, E11 to E13 embryos were removed from pregnant mice under CO_2 anesthesia. The spinal cords were dissected under an Olympus dissection microscope in 4°C HBSS buffer and then digested with 0.1% trypsin at 37°C for 25 minutes. The digested spinal cords were dissociated with glass pipette in HBSS buffer. The cell density was calculated with a hemocytometer under a Zeiss upright microscope. To assay neuronal growth on patterned matrices, 3×10^5 spinal neurons were plated on a 25 mm diameter glass coverslips. The spinal neurons were then cultured in a 37°C incubator with 5% CO_2 for the desired period of time before examination. The hippocampal neurons were prepared from E15 mice. For immunocytochemistry, primary cultured neurons were first fixed with 4% paraformaldehyde, then permeabilized with 0.2% of Triton X-100 in PBS, and finally stained with appropriate primary antibodies. Anti-β3-tubulin antibody (Promega, Madison, WI, USA), a neuronal marker that binds to microtubules, was used to label all neurons. There were no or undetectable glial cells in cultures from E11 spinal cord and E15 hippocampus. The patterned human IgM was shown by fluorescein isothiocyanate (FITC) conjugated anti-human IgM secondary antibodies (Jackson, West Grove, PA, USA), and the nuclei by 4, 6-diamidino-2-phenylindole (DAPI) (Sigma, St Louis, MO, USA). Animal care and the experimental protocols were approved by Mayo Clinic Institutional Animal Care and Use Committee (IACUC) and Research Committee meeting the requirements of the NIH.

Image processing and quantification. Images were collected using an Olympus X70 upright microscope equipped with a 37 Mb digital SPOT camera and processed with Photoshop (Adobe). The total neurite length, outgrowth angle and neuronal attachment were calculated by measuring and quantifying the fluorescence intensity of β3-tubulin or DAPI using Image J software (National Institute of Health). The data were exported and processed with Excel (Microsoft) and analyzed statistically with Prism (Graph-Pad Software Inc., San Diego, CA, USA)[40]. Angular histograms were prepared using Matlab (MathWorks, Natick, MA, USA).

Atomic force microscopy. Atomic force microscopy (AFM) in liquid was carried out on antibody patterns for nanoscale imaging. Contact mode was used with forces less than 800 pN, and multiple scans could be taken without disrupting the sample. The cantilever used was silicon with tip radius of 10 nm and nominal spring constant of 0.03 N/m (MikroMasch, CSC38). The equipment used was an Agilent 5500 with software PicoView 1.8.2 (Agilent Technologies), and analyzed with Gwyddion v2.28 software. Image processing steps include typical 2nd degree polynomial plane subtraction, path leveling, and point correction of a few tip liftoffs for display. Scans were 80×80 μm at 0.5 lines/sec or slower, all done in phosphate buffered saline, pH 7.4.

1. Dickson, B. J. Molecular mechanisms of axon guidance. *Science* **298**, 1959–1964 (2002).
2. Offenhausser, A. *et al.* Microcontact printing of proteins for neuronal cell guidance. *Soft Matter* 290–298 (2007).
3. Keenan, T. M. & Folch, A. Biomolecular gradients in cell culture systems. *Lab Chip* **8**, 34–57 (2008).
4. Park, J. W., Kim, H. J., Kang, M. W. & Jeon, N. L. Advances in microfluidics-based experimental methods for neuroscience research. *Lab Chip* **13**, 509–521 (2013).
5. Hoffman-Kim, D., Mitchel, J. A. & Bellamkonda, R. V. Topography, cell response, and nerve regeneration. *Annu. Rev. Biomed. Eng.* **12**, 203–231 (2010).
6. Sundararaghavan, H. G., Monteiro, G. A., Firestein, B. L. & Shreiber, D. I. Neurite growth in 3D collagen gels with gradients of mechanical properties. *Biotechnol. Bioeng.* **102**, 632–643 (2009).
7. Dotti, C. G., Sullivan, C. A. & Banker, G. A. The establishment of polarity by hippocampal neurons in culture. *J. Neurosci.* **8**, 1454–1468 (1988).
8. Singhvi, R. *et al.* Engineering cell shape and function. *Science* **264**, 696–698 (1994).
9. Fozdar, D. Y., Lee, J. Y., Schmidt, C. E. & Chen, S. Hippocampal neurons respond uniquely to topographies of various sizes and shapes. *Biofabrication* **2**, 035005 (2010).
10. Scholl, M. *et al.* Ordered networks of rat hippocampal neurons attached to silicon oxide surfaces. *J. Neurosci. Meth.* **104**, 65–75 (2000).
11. Chang, J. C., Brewer, G. J. & Wheeler, B. C. Modulation of neural network activity by patterning. *Biosens. Bioelectron.* **16**, 527–533 (2001).
12. Bani-Yaghoub, M. *et al.* Neurogenesis and neuronal communication on micropatterned neurochips. *Biotechnol. Bioeng.* **92**, 336–345 (2005).
13. Yu, L. M., Miller, F. D. & Shoichet, M. S. The use of immobilized neurotrophins to support neuron survival and guide nerve fiber growth in compartmentalized chambers. *Biomaterials* **31**, 6987–6999 (2010).
14. Schroeder, H. W. & Cavacini, L. Structure and function of immunoglobulins. *J. Allergy Clin. Immunol.* **125**, S41–52 (2010).
15. Xu, X. *et al.* A human IgM signals axon outgrowth: coupling lipid raft to microtubules. *J. Neurochem.* **119**, 100–112 (2011).
16. Qin, D., Xia, Y. & Whitesides, G. M. Soft lithography for micro- and nanoscale patterning. *Nat. Protoc.* **5**, 491–502 (2010).
17. Kumar, A. & Whitesides, G. M. Patterned condensation figures as optical diffraction gratings. *Science* **263**, 60–62 (1994).
18. St John, P. M. *et al.* Diffraction-based cell detection using a microcontact printed antibody grating. *Anal. Chem.* **70**, 1108–1111 (1998).
19. Graber, D., Zieziulewicz, T., Lawrence, D., Shain, W. & Turner, J. Antigen binding specificity of antibodies patterned by microcontact printing. *Langmuir* **19**, 5431–5434 (2003).
20. Blattler, T. *et al.* Nanopatterns with biological functions. *J. Nanosci. Nanotechno.* **6**, 2237–2264 (2006).
21. Vogt, A. *et al.* Impact of micropatterned surfaces on neuronal polarity. *J. Neurosci. Meth.* **134**, 191–198 (2004).
22. Moore, K., Macsween, M. & Shoichet, M. Immobilized concentration gradients of neurotrophic factors guide neurite outgrowth of primary neurons in macroporous scaffolds. *Tissue Eng.* **12**, 267–278 (2006).
23. Dertinger, S. K. W., Jiang, X. Y., Li, Z. Y., Murthy, V. N. & Whitesides, G. M. Gradients of substrate-bound laminin orient axonal specification of neurons. *Proc. Natl. Acad. Sci. U.S.A.* **99**, 12542–12547 (2002).
24. Von Philipsborn, A. *et al.* Microcontact printing of axon guidance molecules for generation of graded patterns. *Nat. Protoc.* **1**, 1322–1328 (2006).
25. Mitsunaga, Y. *et al.* Direct evidence that a human antibody derived from patient serum can promote myelin repair in a mouse model of chronic-progressive demyelinating disease. *FASEB J.* **16**, 1325–1327 (2002).
26. Watzlawik, J. *et al.* Human Remyelination Promoting Antibody Inhibits Apoptotic Signaling and Differentiation Through Lyn Kinase in Primary Rat Oligodendrocytes. *Glia* **58**, 1782–1793 (2010).
27. Lander, A. D. Molecules that make axons grow. *Mol. Neurobiol.* **1**, 213–245 (1987).
28. Schmitt, A. M. *et al.* Wnt-Ryk signalling mediates medial-lateral retinotectal topographic mapping. *Nature* **439**, 31–37 (2006).
29. Mukhatyar, V. J. *et al.* Role of fibronectin in topographical guidance of neurite extension on electrospun fibers. *Biomaterials* **32**, 3958–3968 (2011).
30. Vogt, A. K., Lauer, L., Knoll, W. & Offenhausser, A. Micropatterned substrates for the growth of functional neuronal networks of defined geometry. *Biotechnol. Prog.* **19**, 1562–1568 (2003).
31. Fan, L. *et al.* Directional Neurite Outgrowth on Superaligned Carbon Nanotube Yarn Patterned Substrate. *Nano Lett.* **12**, 3668–3673 (2012).
32. LaGraff, J. R. & Chu-LaGraff, Q. Scanning force microscopy and fluorescence microscopy of microcontact printed antibodies and antibody fragments. *Langmuir* **22**, 4685–4693 (2006).
33. Fan, F. R. F. & Bard, A. J. Imaging of biological macromolecules on mica in humid air by scanning electrochemical microscopy. *Proc. Natl. Acad. Sci. U.S.A.* **96**, 14222–14227 (1999).
34. Czajkowsky, D. M. & Shao, Z. The human IgM pentamer is a mushroom-shaped molecule with a flexural bias. *Proc. Natl. Acad. Sci. U.S.A.* **106**, 14960–14965 (2009).
35. Xu, X., Denic, A., Warrington, A. E., Bieber, A. J. & Rodriguez, M. Therapeutics to promote CNS repair: a natural human neuron-binding IgM regulates membrane-raft dynamics and improves motility in a mouse model of multiple sclerosis. *J. Clin. Immunol.* **33 Suppl 1**, S50–56 (2013).
36. Klimovich, V. B. IgM and its receptors: structural and functional aspects. *Biochemistry-Moscow* **76**, 534–549 (2011).
37. Koshland, M. E. The coming of age of the immunoglobulin J chain. *Annu. Rev. Immunol.* **3**, 425–453 (1985).
38. Warrington, A. E. *et al.* Human monoclonal antibodies reactive to oligodendrocytes promote remyelination in a model of multiple sclerosis. *Proc. Natl. Acad. Sci. U.S.A.* **97**, 6820–6825 (2000).
39. Dowell-Mesfin, N. M. *et al.* Topographically modified surfaces affect orientation and growth of hippocampal neurons. *J. Neural Eng.* **1**, 78–90 (2004).
40. Xu, X., Harder, J., Flynn, D. C. & Lanier, L. M. AFAP120 regulates actin organization during neuronal differentiation. *Differentiation* **77**, 38–47 (2009).

Acknowledgements

This work was supported by grants from the NIH (R01 GM092993, R01 NS048357 and R21 NS073684), the National Science Foundation CAREER Award (DBI 1054191), the Minnesota Partnership Award for Biotechnology and Medical Genomics, and the National Multiple Sclerosis Society (CA 1060A). This work was also supported by a High-Impact Pilot and Feasibility Award (HIPFA) and Novel Methodology Award (NMDA) from the Mayo Clinic Center for Translational Science Activities (CTSA) and Mayo Clinic CTSA grant number UL1 TR000135 from the National Center for Advancing Translational

Science (NCATS), a component of the National Institutes of Health (NIH). We also acknowledge with thanks support from the Applebaum, Hilton, Peterson and Sanford Foundations.

Author contributions

X.X., N.J.W., A.E.W., S.-H.O. and M.R. designed experiments. X.X., N.J.W., L.R.J., S.K., J.O.W. and A.E.W. conducted the research. X.X., N.J.W., A.E.W., S.-H.O. and M.R. analyzed data. X.X., N.J.W., S.-H.O. and M.R. wrote the manuscript with input from all coauthors. S.-H.O. and M.R. oversaw the research process.

Additional information

Supplementary information accompanies this paper at http://www.nature.com/scientificreports

Competing financial interests: The authors declare no competing financial interests.

How to cite this article: Xu, X.H. *et al.* A patterned recombinant human IgM guides neurite outgrowth of CNS neurons. *Sci. Rep.* **3**, 2267; DOI:10.1038/srep02267 (2013).